

CFD Simulation of the Effect of Pulsed Jet on the Performance of Liquid-liquid Ejector

Haiyan Bie^a, Chunhong Li^a, Weizhong An^{a,*}, Yaping Jia^a, Jianmin Zhu^b

^aDepartment of Chemistry and Chemical Engineering, Ocean University of China, 238 Songling Road, Qingdao, 266100 China

^bLiaoning Oxiranchem Group, 38 Wanheqi Road, Liaoyang, 111003, China
awzhong@ouc.edu.cn

The aim of this study was to reveal the dynamic characteristics of the liquid-liquid ejector with a pulse current. A three-dimensional ejector model was established. The performances of sucking fluids and mixing performance between the steady ejector and pulsed ejectors with different frequency and amplitude were analyzed. The simulation results showed that the efficiency of the pulsed ejector was higher than that of the steady ejector under the same operating conditions. The ER (entrainment ratio) and η (working efficiency) of the pulsed ejector with higher pulsation amplitude and frequency was much higher than that of the steady ejector. Therefore, it can be concluded that pulsed jet can effectively improve the performances of liquid-liquid ejector.

1. Introduction

Ejector is a kind of fluid machinery and mixing reaction equipment using a high-velocity and high-pressure liquid to pump another low-velocity or low-pressure liquid (Fan et al., 2011). The ejectors have several advantages over the conventional mixing equipment such as no moving parts, no external power required, low maintenance, simple compact and easy to install and applied in various fields (Valery et al., 2013). But the energy lost when the two fluids with different pressure mixed in the ejector is huge. Improving the working efficiency of the ejector has been the focus of scholars around the world.

Many scholars improved the efficiency by optimizing the structure of ejectors. Experimental and numerical studies on the hydrodynamic characteristics of ejector were carried out by Balamurugan et al. (2008). It was found that there was an optimal throat and nozzle area ratio which made the entrainment rate of the suction liquid reach the maximum. Yadav et al. (2008) analyzed the influences of area ratio, suction chamber diameter and contraction angle on the jet coefficient. It was revealed that jet coefficient increased with the increasing of the area ratio, but remained constant when the area ratio increased to the critical value. The liquid entrainment ratio had a peak value when the suction chamber diameter varied within a certain range. Another effective way was to use the unsteady ejector on the same device to improve the efficiency of the ejector, such as pulsed jet, oscillating jet, etc. (Wang and Gao, 2006). The pulsation referred to the operating parameters (such as pressure and flow rate) at any point in the jet flow varied periodically with time in every cycle which called the pulse period. Grosshans et al. (2014) visualized the mixing characteristics of a pulsed jet in a combustion chamber. It was concluded that the pulsed jet enhanced the mixing phenomenon compared to the steady jet. The jet frequency had little effect on the mixing in the spray region but no effect on the mixing in the atomization region. Yadav et al. (2016) investigated the flow structure and mixing characteristics of axisymmetric pulsating jets by PIV method. The length of fully developed zone away from the nozzle exit depended upon the pulsation magnitude and frequency of the pulsed jet. As the pulsation frequency increased, the formation frequency of vortices increased and position of vortice tended to shift toward the nozzle. At present, the research of pulsed ejector was still in the experimental stage and there were few literatures on the study on the mechanism and theory. Although the flow characteristics were still not clear yet, a large number of experimental results revealed that the efficiency of energy transfer and mass transfer of the pulsed jet were higher than that of the steady jet.

In this paper, the flow characteristics of pulsed ejector and steady ejector were analyzed by the numerical simulation. A 3D ejector model was established to investigate the influences of pulsed jet with different frequency and amplitude on the internal flow characteristics and mixing characteristics of liquid-liquid ejector.

2. Geometrical and mathematical models

2.1 Geometries and grids

On the basis of previous achievement (An et al., 2016), the ejector is shown in Figure 1. The main structure of the established ejector model included nozzle, suction chamber, mixer and diffuser (Aimal et al., 2013). The parameters of the ejector are listed in Table 1. The ejector was divided into four parts, because of the complex structure of the suction chamber, the unstructured grid was used in this part. And the structured grid was used to meshing the other parts. The grids of the jet core region and mixing section were refined. The grids of the ejector are shown in Figure 2.

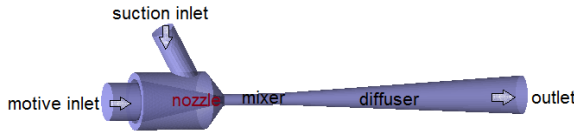


Figure 1: Schematic diagram of the ejector.

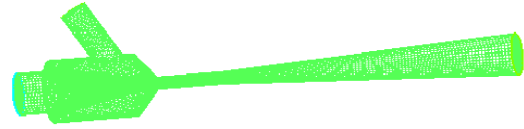


Figure 2: Grids of the ejector.

Table 1: The dimension of the ejector

Parameters	Values	Parameters	Values
Motive inlet diameter (mm)	40	Throat diameter (mm)	12
Suction inlet diameter (mm)	25	Mixing section (mm)	60
Nozzle diameter (mm)	7	Diffusion angle (°)	3°

2.2 The governing equations and boundary conditions

2.2.1 The governing equations

The mass conservation equation:

$$\frac{\partial \rho}{\partial t} + \text{div}(\rho \vec{u}) = 0 \quad (1)$$

where ρ is density; \vec{u} is velocity vector of fluid.

The momentum conservation equation:

$$\frac{\partial(\rho u_i)}{\partial t} + \frac{\partial(\rho u_i u_j)}{\partial x_j} = -\frac{\partial p}{\partial x_i} + \frac{\partial}{\partial x_j} \left[u \left(\frac{\partial u_i}{\partial x_j} + \frac{\partial u_j}{\partial x_i} \right) \right] - \frac{2}{3} \frac{\partial}{\partial x_i} \left[\delta_{ij} \left(\rho k + \mu \frac{\partial u_k}{\partial x_k} \right) \right] \quad (2)$$

where k is heat transfer coefficient of the fluid; p is pressure.

The energy conservation equation:

$$\frac{\partial}{\partial t}(\rho T) + \text{div}(\rho \vec{u} T) = \text{div} \left(\frac{k}{c_p} \text{grad} T \right) + S_T \quad (3)$$

where T is temperature; S_T is viscous dissipation term; c_p is specific heat capacity at constant pressure.

The species conservation equation:

$$\frac{\partial(\rho c_s)}{\partial t} + \text{div}(D_s \cdot \text{grad}(\rho c_s)) + S_s \quad (4)$$

where C_s is the volume concentration of component s , D_s is the diffusion coefficient, and S_s is the productivity within the system.

The fluid in the simulation was assumed incompressible. Standard k - ϵ model was chosen and the turbulence kinetic energy k and the specific dissipation rate ϵ can be obtained from the following transport equations:

$$\frac{\partial(\rho k)}{\partial t} + \frac{\partial(\rho k u_i)}{\partial x_i} = \frac{\partial}{\partial x_j} \left[\left(\mu + \frac{\mu_t}{\sigma_k} \right) \frac{\partial k}{\partial x_j} \right] + \mu_t \left(\frac{\partial u_i}{\partial x_j} + \frac{\partial u_j}{\partial x_i} \right) - \rho \varepsilon \quad (5)$$

$$\frac{\partial(\rho \varepsilon)}{\partial t} + \frac{\partial(\rho \varepsilon u_i)}{\partial x_i} = \frac{\partial}{\partial x_j} \left[\left(\mu + \frac{\mu_t}{\sigma_k} \right) \frac{\partial \varepsilon}{\partial x_j} \right] + C_{1\varepsilon} \frac{\varepsilon}{k} (G_k + C_{3\varepsilon} G_b) - C_{2\varepsilon} \rho \frac{\varepsilon^2}{k} \quad (6)$$

$$\mu_t = \rho C_\mu \frac{k^2}{\varepsilon} \quad (7)$$

where μ_t is turbulent viscosity; G_b is the generation item of turbulent kinetic energy k and for the incompressible fluid, $G_b = 0$.

2.2.2 Boundary conditions

Both motive and suction inlets were selected as the pressure-inlet boundary while the outlet of the ejector was selected as the pressure-out boundary. The inlet pressure of the steady ejector was set to be 0.3 MPa, and the initial pressure of pulsed ejectors was also set to be 0.3 MPa. The function of UDF was used to define the pressure of motive fluid with different pulsation frequency and amplitude. The pulse parameters of the motive fluid are shown in Table 2. In order to ensure the convergence precision, the momentum equation, the turbulent kinetic energy and turbulence dissipation rate equations were all solved using the second-order upwind difference scheme. The SIMPLE algorithm was adopted in the coupling of pressure and velocity. In the simulation, the two kinds of fluids were water and ethanol, and the water was the motive fluid, the ethanol was suction fluid.

Table 2: The pulse parameters of the motive fluid of the pulsed ejector

Ejector type	Change Period (s)	Frequency (Hz)	Amplitude (MPa)
A	0.2	5	0.1
B	0.4	2.5	0.1
C	0.2	5	0.15
D	0.4	2.5	0.15
E	0.2	5	0.05
F	0.4	2.5	0.05
G	--	--	--

3. Results and discussions

In order to investigate the effects of pulsed jet on the performance of the ejector, a series of simulations were finished based on the present geometrical and mathematical models. In addition, the influences of pulsation frequency and amplitude on the performance of the pulsed ejector were also studied. The results were summarized as follows:

3.1 Mass fraction on outlet and jet centerline

Figure 3 shows the variation of the mass fraction of suction fluid at the outlet of ejectors with time. It can be seen that the mass fraction of the suction fluid increased along with the flow time. The mass fraction of suction fluid on the outlet interface was cyclical with the change of the motive fluid pressure. And the mass fraction of the suction fluid on the outlet interface of pulsed ejectors was higher than that of the steady ejector. Especially at $t = 0.4$ s, 0.8 s, 1.2 s, 1.6 s (while the inlet pressure of the motive fluid was the same as that of the pulsed ejector and steady ejector), the mass fractions of pulsed ejectors were still higher than that of steady ejector.

The mass fraction of suction fluid along the jet centerline at $t = 1.6$ s is shown in Figure 4. It can be seen that the mass fraction of suction fluid was zero at the position where the nozzle located, after the motive fluid jetted out from nozzle, the mass fraction increased gradually as the suction fluid was sucked into the jet core region. It can be seen that the instantaneous mass fraction of the pulsed ejector was higher than that of the steady ejector at any position, which indicated that pulsed ejectors sucked more fluid than steady ejector under the same working pressure. The suction fluid mass fraction of ejector with the frequency of 5 Hz and amplitude of 0.15 MPa was higher than that of the other ejectors, which indicated that the pulsed ejector with high amplitude and high frequency sucked more fluid. By comparing curve A with B (C and D or E and F), it can be concluded that the performance of ejectors with higher pulsation frequency was better than that of the ejectors

with the same pulse amplitude. By comparing curve A, C and E, it can also be concluded that ejectors with a larger amplitude had better ability of sucking fluid over other pulsed ejectors with the same frequency.

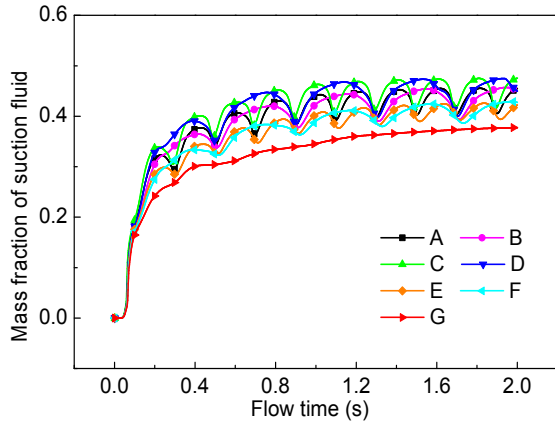


Figure 3: The mass fraction of suction fluid at outlet of ejectors with time.

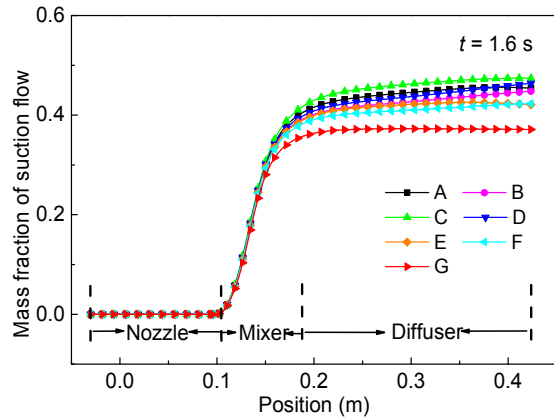


Figure 4: The mass fraction of suction fluid along the jet centerline at $t = 1.6$ s.

3.2 Entrainment Ratio

Entrainment Ratio (ER) is one of the most important performances of ejector. The value of ER is the ratio of the mass flow rate of the suction fluid to the motive fluid. Figure 5 shows the ER at different flow time. It can be seen that the ER of pulsed ejectors are higher than that of the steady ejector along with the flow time and frequency of ER varied with the pressure of motive fluid. Besides, the peak and valley value of ER are delayed or advanced correspondingly due to the change of pulsation frequency. The magnitude of the amplitude also has a corresponding effect on ER.

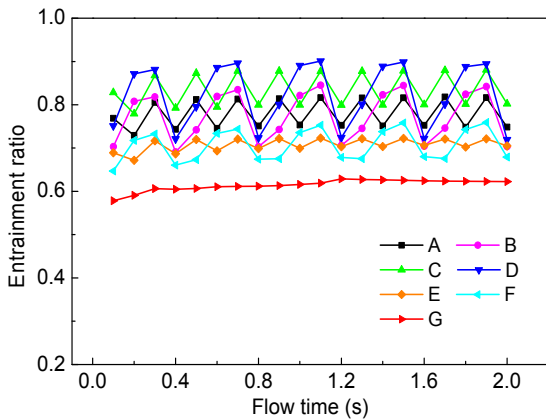


Figure 5: ER at different flow time.

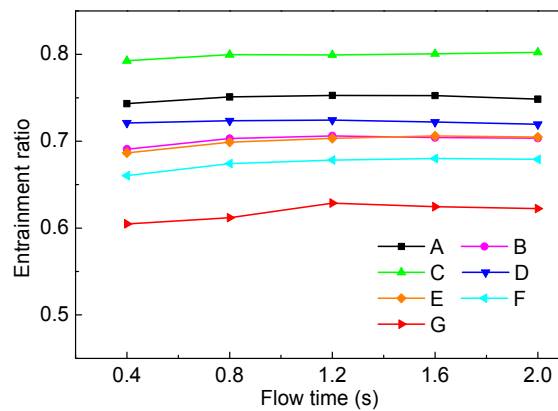


Figure 6: ER of different ejectors under the same pressure of motive fluid.

Figure 6 shows ER of the ejectors at time of 0.4 s, 0.8 s, 1.2 s, 1.6 s. It can be seen that the ranking of ER was $C > A > D > B > E > F > G$, which indicating that the performances of the pulsed ejectors were better than that of the steady ejector at the same pressure. The ejector with the frequency of 5 Hz and amplitude of 0.15 MPa sucked more suction fluid than others. One of the reasons was that the periodic variation of the pressure caused disturbance in the pulsed ejector. In other word, when the working pressure returned to the equilibrium value, the turbulence intensity along the jet centre of the pulsed ejector was still stronger than that of the steady ejector. Therefore, it can be concluded that the ER of ejector with higher pulsation frequency was bigger than the others with the same pulse amplitude. The larger the amplitude was, the higher the ER of the ejector was.

3.3 Working efficiency

Working efficiency is the overall performance of the ejector. It can be expressed by Eq(8),

$$\eta = u \frac{\Delta p_c}{\Delta p_p - \Delta p_c} \quad (8)$$

where Δp_c was the pressure difference between the outlet fluid and suction fluid, Δp_p was the pressure difference between the motive fluid and the suction fluid.

Working efficiency at different time (the pressure of motive fluid was equal to each other) is shown in Table 3. It can be seen that the ranking of η was C>A>D>B>E>F>G. Therefore, the working efficiency of pulsed ejector was better than that of steady ejector. And the working efficiency of pulsed ejector can be enhanced by increasing the pulsation frequency and amplitude.

Table 3: Working efficiency at different time of the pulsed ejectors and the steady ejector

Ejector	Working efficiency (%)				
	$t=0.4$ s	$t=0.8$ s	$t=1.2$ s	$t=1.6$ s	$t=2.0$ s
A	37.76	38.16	38.25	38.24	38.02
A	37.76	38.16	38.25	38.24	38.02
B	35.02	35.64	35.81	35.70	35.66
C	40.36	40.73	40.72	40.78	40.87
D	36.59	36.72	36.76	36.64	36.50
E	34.76	35.39	35.61	35.75	35.69
F	33.46	34.18	34.39	34.49	34.44
G	30.56	30.93	31.79	31.57	31.46

3.4 Internal flow field

In order to reveal the flow characteristics inside the ejectors, mass fraction and velocity were analyzed. The mixing characteristics of the two fluids in the ejector are shown in Figure 7. It can be seen that a mixed boundary layer was formed between the two fluids due to the concentration difference. Then the mass fraction of the motive fluid decreased gradually. In this process, the thickness of the mixed boundary layer increased gradually, and the concentration gradient became smaller and smaller. After a certain distance, the concentration difference reduced to zero, which meaning that the two fluids mixed evenly eventually. The mixing of the two fluids mainly happened in the mixing section.

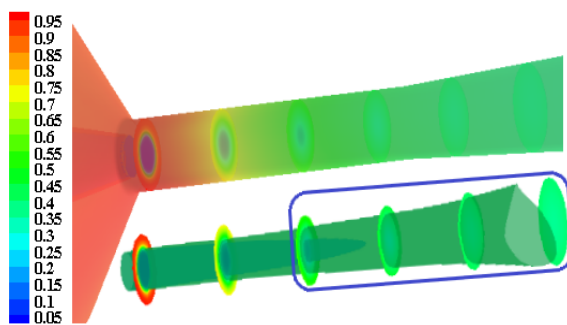


Figure 7: The mass fraction of suction flow in mixing section.

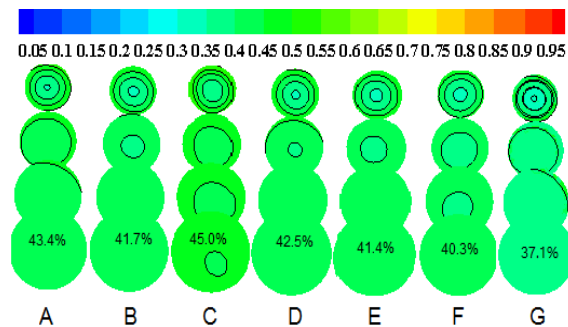


Figure 8: The mass fraction of suction fluid at different position of nozzle exit.

The mixing performance was also very important for ejector. Several positions marked in Figure 7 were selected to analyse the mixing performance of the ejectors. It can be seen from Figure 8 that the concentration difference between two fluids in the ejector E and ejector B reduced much more quickly than others. Mass fraction of ejector C was higher than that of the others at the same position, but there was still a large concentration difference in the mixing section. Comparatively speaking, the mixing performance of ejector D was better than the other ejectors. It can be concluded that the frequency and amplitude of motive pressure had great influence on the mixing performance of the ejector. Only the frequency and amplitude matched well with the size of the ejector can make the ejector acquire high mixing performance. Several ejectors were

selected randomly to study the mechanism of improving the entrainment performance of ejector by pulsed jet. Figure 9 shows the velocity distribution on axial section of different ejectors. It can be seen that two fluids mixed well mainly due to the existence of turbulence core in mixing section. L/D is the length of turbulent core to the nozzle diameter which represents the relative length of the turbulent core. The longer the length of the turbulent core was, the longer distance of mixing fluids was needed. As the pulsed ejector had much variability of the working condition, the ejector has not been completely stable at the end of the previous working cycle, the next working cycle has already started. So the turbulence intensity along the jet center of the pulsed ejector was larger than that of the steady ejector. And the turbulence intensity increased with the increasing of the pulsation frequency and amplitude. Besides, the entrainment and diffusivity of the pulsed ejectors were also enhanced. Because the pulsed jet had a strong diffusion, a longer mixing distance was also required for the pulsed ejector. Therefore, pulsation frequency and amplitude had a great influence on the performance of the pulsed ejector.

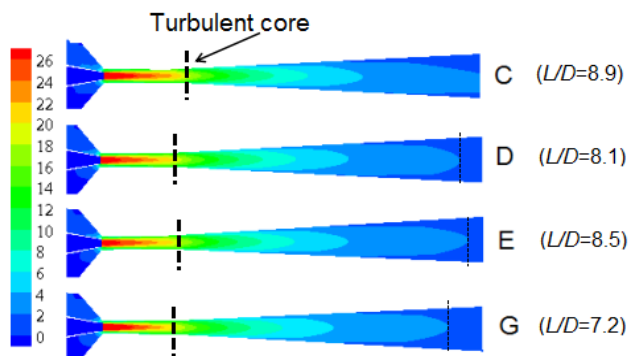


Figure 9: Velocity distribution on axial section and relative length of turbulent core of different ejectors.

4. Conclusions

In this paper, the dynamic characteristics of the pulsed ejector and the steady ejector were analyzed. By comparing the entrainment performance and mixing effect of these ejectors, it was concluded that pulsed ejectors had better performances of sucking fluid than that of the steady ejector under the same operating conditions. The ER and working efficiency increased with the increasing of the pulsation frequency and amplitude. Adopting pulsed jet was an effective way to improve the performances for liquid-liquid ejector. It was also revealed that turbulence intensity along the jet center of pulsed ejector was larger than that of the steady ejector. Higher pulsation frequency and amplitude can cause larger turbulence intensity. Turbulence intensity made pulsed ejectors had high rate of entrainment and diffusivity.

References

- Ajmal S., Imran R C., Mansoor H I., 2013, Experimental Study of the Characteristics of Steam Jet Pump and Effect of Mixing Section Length on Direct-contact Condensation, *International Journal of Heat and Mass Transfer*, 58, 62-69.
- An W Z., Bie H Y., Liu C C., Hao Z R., 2016, CFD Simulation on the Turbulent Mixing Flow Performance of the Liquid-liquid Ejector, *Materials Science and Engineering*, 129(1), 12005-12012.
- Balamurugan S., Gaikar V G., Patwardhan A W., 2008, Effect of Ejector Configuration on Hydrodynamic Characteristics of Gas-liquid Ejectors, *Chemical Engineering Science*, 63, 721-731.
- Fan J., Eves J., Thompson H M., Toropov V V., Kapur N., Copley D., Mincher A., 2011, Computational Fluid Dynamic Analysis and Design Optimization of Jet Pumps, *Computers & Fluids*, 46, 212-217.
- Grosshans, H., Szasz, R.Z., Funchs, L., 2014, Enhanced Liquid Gas Mixing Due to Pulsating Injection, *Comput Fluids*, 107, 196-204.
- Wang L H., Gao C C., 2006, Study Progress of Pulsed Jet Pump, *Water Conservancy & Electric Machinery*, 06, 33-35.
- Valery Z., Egon H., Nikolai K., 2013, Influence of Issued Jet Conditions on Mixing of Confined Flows, *Chemical Engineering Transactions*, 32, 1459-1464.
- Yadav H., Agrawa A., Srivastava A., 2016, Mixing and Entrainment Characteristics of a Pulse Jet, *International Journal of Heat and Fluid Flow*, 61, 749-761.
- Yadav R L., Patwardhan A W., 2008, Design Aspects of Ejectors: Effects of Suction Chamber Geometry, *Chemical Engineering Science*, 63, 3886-3897.